Mon. Not. R. Astron. Soc. **000**, 000–000 (0000) Printed 5 February 2008 (MN LATEX style file v2.2)

The Effect of Gravitational Recoil on Black Holes Forming in a Hierarchical Universe

Noam I. Libeskind[1], Shaun Cole[1], Carlos S. Frenk[1], & John C. Helly[1]

[1] *Department of Physics, University of Durham, Science Laboratories, South Road, Durham, DH1 3LE, U.K.*

5 February 2008

ABSTRACT

Galactic bulges are known to harbour central black holes whose mass is tightly correlated with the stellar mass and velocity dispersion of the bulge. In a hierarchical universe, galaxies are built up through successive mergers of subgalactic units, a process that is accompanied by the amalgamation of bulges and the likely coalescence of galactocentric black holes. In these mergers, the beaming of gravitational radiation during the plunge phase of the black hole collision can impart a linear momentum kick or "gravitational recoil" to the remnant. If large enough, this kick will eject the remnant from the galaxy entirely and populate intergalactic space with wandering black holes. Using a semi-analytic model of galaxy formation, we investigate the effect of black hole ejections on the scatter of the relation between black hole and bulge mass. We find that while not the dominant source of the measured scatter, they do provide a significant contribution and may be used to set a constraint, $v_{\rm kick} \lesssim 500\,{\rm km\,s^{-1}}$, on the typical kick velocity, in agreement with values found from general relativistic calculations. Even for the more modest kick velocities implied by these calculations, we find that a substantial number of central black holes are ejected from the progenitors of present day galaxies, giving rise to a population of wandering intrahalo and intergalactic black holes whose distribution we investigate in high-resolution N-body simulations of Milk-Way mass halos. We find that intergalactic black holes make up only $\sim 2-3\%$ of the total galactic black hole mass but, within a halo, wandering black holes can contribute up to about half of the total black hole mass orbiting the central galaxy. Intrahalo black holes offer a natural explanation for the compact X-ray sources often seen near the centres of galaxies and for the hyperluminous non-central X-ray source in M82.

1 INTRODUCTION

The discovery that galactic bulges harbour supermassive black holes whose masses are correlated with the properties of the bulge suggests a close connection between the formation of galaxies and the formation of black holes. The mass of the galactocentric black hole varies approximately linearly with the stellar mass of the bulge (Kormendy & Richstone 1995; Magorrian et al. 1998; McLure & Dunlop 2002) and roughly as the fourth power of the bulge velocity dispersion (Ferrarese & Merritt 2000, Gebhardt et al. 2000, Tremaine et al. 2002). Correlations with the near infrared bulge luminosity (Marconi & Hunt 2003) and with the bulge light concentration (Graham et al. 2001) have also been found. These correlations are remarkable because they link phenomena on widely different scales - from the parsec scale of the black hole's sphere of influence to the kiloparsec scale of bulges - and thus point to a connection between the physics of bulge formation and the physics of black hole accretion and growth (Milosavljevic & Merritt 2001). The simplest interpretation is that both, black hole and bulge growth, are driven by the same process whose nature, however, remains unclear.

Various models for the growth of black holes in galaxies have been studied (e.g. Haehnelt & Rees 1993; Silk & Rees 1998; Cattaneo, Haehnelt & Rees 1999; Kauffmann & Haehnelt 2000; Ostriker 2000; Volonteri, Haardt & Madau 2002; Di Matteo, Springel & Hernquist 2005, and others). In the context of a hierarchical cold dark matter universe, a plausible explanation for the tight correlation between bulge and black hole properties is that the galaxy mergers or disc instabilities that induce bulge growth via bursts of star formation also feed the central black hole (Kauffmann & Haehnelt 2000; Croton et al. 2005; Bower et al. 2005.) A simple implementation of this model follows from assuming that, as cold gas condenses into stars, a certain percentage of the gas is forced into the centre of the galaxy and accreted by the black hole. Models based on this and related prescriptions successfully reproduce the $m_{\rm BH}-m_{\rm b}$ relation (hereafter we use this term to refer to the relation between black hole mass and stellar bulge mass)

(Croton et al. 2005; Bower et al. 2005; Malbon in prep 2005).

An interesting aspect of the correlations between black hole mass and bulge properties is that they seem to apply over a range of five to six orders of magnitude in black hole mass (Tremaine et al. 2002; Gebhardt, Rich & Ho 2002). If a simple model of the kind just mentioned for the simultaneous growth of black holes and bulges is correct, then there are two direct consequences which we explore in this paper. The first is that black holes should exist in bulges of all luminosities including dwarf ellipticals and satellites of brighter galaxies like the Milky Way. The second is that black holes will likely merge as their hosts bulges collide.

Binary black holes orbiting each other emit gravitational waves (Peters & Matthews 1963). Using quasi-Newtonian methods to study the orbital decay due to gravitational wave emission, Fitchett (1983) found that the system will eventually enter a plunge phase, causing the black holes to coalesce emitting a burst of gravitational waves. Peres (1962) found that, in addition to transferring energy out of the emitting system, gravitational radiation can also take with it linear momentum. As a result, the centre of mass of the system recoils in a direction specified by the boundary conditions of the last stable orbit.

The astrophysical implication of this linear momentum kick (the "rocket effect" or "gravitational recoil") is that black holes may be ejected from galactic bulges if the potential is shallow and the kick is large enough (Madau & Quataert 2004; Merritt et al. 2004; Enoki et al. 2004). In theory, this could lead to a sizable population of extragalactic black holes which could, in principle, dominate the black hole mass function. Our aim in this work is to examine the importance of such kicks for the galactic black hole population. In particular, we consider the scatter on the $m_{\rm BH} - m_{\rm b}$ relation in an attempt to constrain the relatively uncertain kick velocity, as well as the nature and spatial distribution of a possible extragalactic population of ejected black holes. We model the growth of black holes using the semi-analytic galaxy formation model of Cole et al. (2000), using two methods for obtaining merger trees: Monte Carlo techniques and high resolution N-body simulations (in which the trajectories of recoiling black holes can be tracked.)

This paper is organised as follows. In section 2, we review the physics of the gravitational recoil. In section 3, we describe how we model the formation and ejection of black holes in our semi-analytic model. In section 4, we determine the effect of black holes ejected from the progenitors of present day galaxies on the $m_{\rm BH} - m_{\rm b}$ relation. In section 5, we use a set of high resolution N-body simulations of galactic halos to track the location of ejected black holes. We conclude in Section 6 where we discuss the possible consequences of an extragalactic black hole population.

2 THE PHYSICS OF KICKS

The emission of gravitational radiation is a generic feature of any massive asymmetrically collapsing system (Peres 1962). In order to be accompanied by a linear momentum kick, the gravitational radiation must be asymmetric (Fitchett 1983). For two coalescing black holes of unequal mass this occurs as the gravitational radiation from the lighter, more rapidly moving partner is more strongly beamed. As two black holes orbit each other, gravitational radiation causes their orbits to shrink and circularise until the last stable circular orbit is reached. Using perturbation theory in the weak field approximation, Fitchett (1983) calculated the kick velocity from this final orbit to be:

$$v_{\rm kick} = 1480 \left(\frac{f(q)}{f_{\rm max}}\right) \left(\frac{2G(m_1+m_2)/c^2}{r_{\rm isco}}\right)^4 \,{\rm km\,s^{-1}} \qquad (1)$$

where $r_{\rm isco}$ is the radius of the innermost stable circular orbit, $q \equiv m_1/m_2$ is the mass ratio with the convention $m_2 > m_1$, and $f(q) = q^2(1-q)/(1+q)^5$ which reaches a maximum, $f_{\rm max} = 0.0179$, for a mass ratio of $q_{max} \approx 0.382$. Unfortunately, the weak field approximation used by Fitchett becomes invalid as the binary approaches the plunge phase and it is here that the contribution to the recoil velocity becomes largest.

Two decades later, Favata, Hughes & Holz (2004) used perturbation theory to show that, in the presence of strong fields, gravitational kicks are not expected to exceed $600\,{\rm km\,s^{-1}}$. In a companion paper, Merritt et al. (2004) included the effect of the larger partner's spin and obtained an upper limit of $\sim 500\,{\rm km\,s^{-1}}$. More recently Blanchet, Qusailah & Will (2005) performed a higher order calculation of the recoil for the special case of the coalescence of two non-rotating black holes, obtaining an upper limit of $300\,{\rm km\,s^{-1}}$. However, none these calculations apply to all mass and spin ratios and kick velocities as large as $1000\,{\rm km\,s^{-1}}$ cannot be definitively ruled out.

In light of the uncertainty in the recoil velocity, we simply assume that the kick is directly proportional to Fitchett's scaling function $f(q)$ and write the recoil velocity in terms of a prefactor velocity $v_{\rm pf}$,

$$v_{\rm kick} = v_{\rm pf} \frac{f(q)}{f_{\rm max}}. \qquad (2)$$

We then allow $v_{\rm pf}$ to vary between $0\,{\rm km\,s^{-1}}$ (i.e. no kick) to $1000\,{\rm km\,s^{-1}}$ with the aim of constraining this parameter empirically.

3 THE GALFORM SEMI-ANALYTIC MODEL

In this section, we briefly explain how we use the semi-analytic galaxy formation model GALFORM described in detail by Cole et al. (2000), Benson et al. (2002) and Bower et al. (2005) to model the growth and evolution of galaxies. The growth of dark matter halos by mergers is encoded in a merger tree. Along each branch of the tree, the following physical processes are calculated: (i) shock-heating and virialization of gas within the gravitational potential well of each halo; (ii) radiative cooling of gas onto a galactic disc; (iii) the formation of stars from the cooled gas; (iv) the effects of photoionization on the thermal state and cooling properties of the intergalactic medium; (v) reheating and expulsion of cooled gas through feedback processes associated with stellar winds and supernovae explosions (see Benson et al. 2003); (vi) the evolution of the stellar populations; (vii) the effects of dust absorption and radiation; (viii) the chemical evolution of the stars and gas; (ix) galaxy mergers (which, depending on the violence of the merger, may be accompanied by starbursts and the formation of a

bulge – see Baugh et al. 1998); (x) the evolution of the size of the disc and bulge.

We used two different methods for obtaining dark matter halo merger trees. In the first instance, we constructed the trees using a Monte-Carlo algorithm to determine merger rates (e.g. Lacey & Cole 1993, Cole et al. 2000). In the second instance, we explicitly extracted the merger trees by following the merging of dark matter halos in N-body simulations (Helly et al. 2003). The latter method allows us to apply the semi-analytic formalism directly to the simulations. More details are given in Section 5.2.

3.1 Discs

Stellar discs are formed as rotating diffuse halo gas cools and settles in a halo. In the GALFORM model, discs are assumed to have an exponential surface density profile,

$$\Sigma(r) = \Sigma_{\rm D} \exp\left(\frac{-r}{r_{\rm D}}\right), \tag{3}$$

where $r_{\rm D}$ is a characteristic disc length and $\Sigma_{\rm D}$ is the central surface density. The potential of such a mass distribution as a function of just radius (i.e. in the plane of the disc) is

$$\phi(r, z=0) = -\pi G \Sigma_{\rm D} r [I_0(y)K_1(y) - I_1(y)K_0(y)] \tag{4}$$

where $y \equiv r/2r_{\rm D}$. The functions $I_n(y)$ and $K_n(y)$ are modified Bessel functions of the first and second kind (e.g. Binney & Tremaine 1987). Differencing the potential at $r = 0$ and $r = \infty$, we find that the escape velocity from the centre of the disc is

$$v^2_{\rm D,esc} = 3.36\,\frac{GM_{\rm D}}{r_{\rm D,1/2}}, \tag{5}$$

where $r_{\rm D,1/2}$ is the half mass radius of the disc.

3.2 Bulges

In the GALFORM model, the principal mechanism for forming both elliptical galaxies and the bulges of luminous spiral galaxies is galaxy mergers. When two galaxies of comparable mass merge, this is termed a major merger and all the stars from both merging partners are assumed to form a single spheroid while any gas present is consumed in a burst of star formation. In minor mergers there is no burst of star formation; only the stars from the smaller galaxy are added to the bulge of the larger galaxy, while the gas is added to the disc of the larger galaxy.

In the context of the GALFORM model, Cole et al. (2000) also considered the possibility that dynamical instability in selfgravitating discs could result in the formation of galactic bulges (see also Mo, Mao & White (1998)). They found that this mechanism was unlikely to contribute significantly to the formation of large bulges, but could be important in creating the bulges of lower luminosity galaxies. The criterion they used to determine whether a cold disc was unstable was $\epsilon_{\rm m} lsim \epsilon_{\rm m}^{\rm crit} = 1.1$, where

$$\epsilon_{\rm m} = \frac{V_{\rm max}}{(GM_{\rm disc}/r_{\rm D,1/2})^{1/2}} \tag{6}$$

(Efstathiou, Lake & Negroponte 1982). Here $V_{\rm max}$ is the circular velocity at the disc half-mass radius, $r_{\rm D,1/2}$. We adopt the slightly lower value of $\epsilon_{\rm m}^{\rm crit} = 1.05$ in order to obtain a distribution of bulge to total luminosities similar to that found in the Sloan Digital Sky Survey by Tasca & White (2005). For such unstable discs it was assumed that all the disc stars would be transformed into bulge stars and any cold disc gas would undergo a burst of star formation. The assumption that bulges, and as we discuss later, black holes grow as a result of discs becoming unstable is also assumed in the AGN feedback models incorporated in the latest semi-analytic models of Croton et al. (2005) and Bower et al. (2005). To illustrate the importance of this mechanism, we present models both with and without this secondary route for generating galactic bulges.

The density profile we adopt for bulges is the Hernquist (1990) model,

$$\rho(r) = \frac{M_{\rm B}}{2\pi}\,\frac{a}{r}\,\frac{1}{(r+a)^3}, \tag{7}$$

where a is a scale length and $M_{\rm B}$ is the total bulge mass. The potential of such a profile is found by integrating the Poisson equation and the escape velocity from the centre of such a spheroid is given by

$$v^2_{\rm B,esc} = 4.83\,\frac{GM_{\rm B}}{r_{\rm B,1/2}}, \tag{8}$$

where $r_{\rm B,1/2}$ is the bulge's half mass radius.

3.3 Black Holes

We assume that the growth of black holes is proportional to the growth of bulges. Whenever an event that adds stellar mass to the bulge occurs, we assume that a fraction, $f_{\rm BH}$, of that mass is accreted by the central black hole. This assumption is motivated in part by models of black hole growth such as that of Kauffmann & Haehnelt (2000), wherein black holes accrete a proportion of the cold gas being consumed in a burst of star formation. In our model, black holes grow both as a result of such star formation bursts *and* also by the accretion of stars in mergers or as the result of disc instabilities. We assume that in each case the same mass fraction, $f_{\rm BH}$, is channelled onto the black hole. This simplifying assumption has the virtue that, in the absence of black hole ejection, all bulges will have black holes that sit precisely on the $m_{\rm BH} - m_{\rm b}$ relation and so we can, in principle, use the scatter induced by black hole ejections to set a firm upper limit on the kick velocities. The precise value of $f_{\rm BH}$ needed to match the data has changed in the literature (e.g. see Magorrian et al. 1998; Merritt et al. 2004) and we choose $f_{\rm BH} = 0.001$, the value published by McLure & Dunlop (2002) from estimates of black hole masses for 72 active galaxies.

During a merger, we assume that a fraction of any new stellar bulge mass is added to the existing black hole,

$$M_{\rm BH,\ new} = M_{\rm BH,\ old} + f_{\rm BH}\,\Delta M_{\rm bulge}. \tag{9}$$

If the black hole is ejected during the merger, we assume that a new black hole is born whose mass is equal to the mass fraction that would have been added to the preexisting black hole had it not been ejected, that is:

$$M_{\rm BH,\ new} = f_{\rm BH}\,\Delta M_{\rm bulge}. \tag{10}$$

This black hole then becomes the focus of mass accretion during subsequent episodes of bulge growth. In this way,

we ensure that all bulges contain a black hole at all times and that, in the absence of gravitational recoil, all black holes at all times have masses directly proportional to their bulges and hence lie on a perfect $m_{\rm BH} - m_{\rm b}$ relation with zero scatter. The implicit assumption that black holes exist only in bulges and not in discs, and that black holes grow during mergers rather than during quiescent star formation is motivated simply by the desire to reproduce the empirical $m_{\rm BH} - m_{\rm b}$ relation.

We assume that once two galaxies have merged, their central black holes coalesce instantaneously. This should be a good approximation as the black holes will merge on a dynamical timescale while the time between galaxy mergers, which is determined by the hierarchical growth of structure, is typically much longer. Note that even when the merger rate of dark matter halos is relatively high, the galaxies orbiting inside the dark halos will only merge once their orbits decay due to energy loss by dynamical friction against the halo material (Lacey & Cole 1993). This implies that three-body mergers in which ejections could occur via a slingshot effect (e.g. Saslaw, Valtonen, & Aarseth 1974) are expected to be rare.

The mass ratio of the merging black holes determines the recoil velocity, $v_{\rm kick}$, according to equation (2). Thus, to determine whether the recoiling black hole escapes from the galaxy we add the bulge and disc potentials and require

$$v_{\rm kick}^2 > v_{\rm esc}^2 \equiv 3.36\,\frac{GM_{\rm D}}{r_{\rm D,1/2}} + 4.83\,\frac{GM_{\rm B}}{r_{\rm B,1/2}}. \qquad (11)$$

Note that we neglect the contribution of the dark matter halo. This is a good approximation over the lengthscale of the galaxy because the dark matter potential has a very shallow gradient. However, the dark matter potential becomes increasingly important for black holes that escape the galaxy and, in Section 5.2, we use an alternative method to follow their orbits. If the recoil velocity, $v_{\rm kick}$, is less then $v_{\rm esc}$ we assume that the black hole will not escape but rapidly return to the centre of the galaxy. This should be a good approximation: according to the calculations of Madau & Quataert (2004), recoiling black holes that have insufficient kinetic energy to escape undergo damped oscillations about the galactic nucleus which decay in a few dynamical times.

Our modelling of black hole growth thus automatically reproduces an empirical $m_{\rm BH} - m_{\rm b}$ relation. If the prefactor velocity, $v_{\rm pf}$, in equation (2) is zero, the black hole masses are all directly proportional to the bulge mass of their host galaxies. If $v_{\rm pf}$ is not zero, gravitational kicks introduce scatter in the $m_{\rm BH} - m_{\rm b}$ relation which we now investigate and compare with observations.

4 THE EFFECT OF VELOCITY KICKS ON THE $m_{\rm BH} - m_{\rm b}$ RELATION

In order to investigate how the $m_{\rm BH} - m_{\rm b}$ relation is affected by the ejection of recoiling black hole merger remnants we have studied a sample of 1000 halos of final mass $10^{12} M_{\odot}$. Merger trees for each halo were generated using the Monte-Carlo method described by Cole et al. (2000) and the `GALFORM` rules of galaxy formation were applied to each branch of the tree. The growth of each central black hole (which tracks the growth of the bulge) was calculated as described in Section 3.3. Our fiducial model includes the process of bulge formation by disc instability discussed in Section 3.2. For every black hole merger we consider kick velocities corresponding to values of the prefactor, $v_{\rm pf}$, in eqn (2) in the range 0 - 1000 $\rm km\,s^{-1}$.

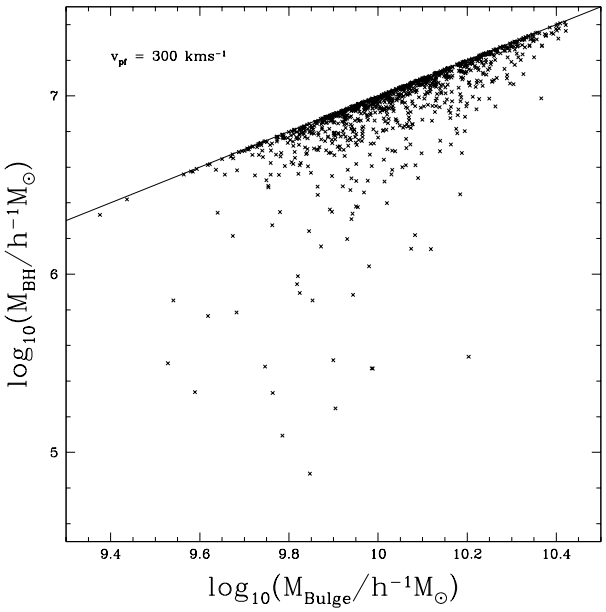

Figure 1. The $z = 0$ $m_{\rm BH} - m_{\rm b}$ relation for the case in which black hole merger remnants have the kick velocity given by equation (2) with $v_{\rm pf} = 300$ $\rm km\,s^{-1}$. The diagonal line represents the 'ideal' $m_{\rm BH} - m_{\rm b}$ relation for which $M_{\rm BH}/M_{\rm bulge} = f_{\rm BH} = 10^{-3}$.

The ejection of a black hole from the bulge is a source of scatter in the $m_{\rm BH} - m_{\rm b}$ relation. Fig. 1 shows the $z = 0$ $m_{\rm BH} - m_{\rm b}$ relation for 1000 halos assuming a moderate prefactor kick velocity of 300 $\rm km\,s^{-1}$. Note that black hole mass may only be scattered downwards by ejections. Galactic bulges that have never experienced an ejection lie exactly on the diagonal line.

In the absence of kicks, the model, by definition, gives a perfect $m_{\rm BH} - m_{\rm b}$ relation with no scatter. As the kick velocity increases, a tail of bulges that host black holes of reduced mass appears, while the remaining galaxies whose progenitors never lost their black hole still lie precisely on the relation. The form of the scatter about the $m_{\rm BH} - m_{\rm b}$ relation and its dependence on the prefactor $v_{\rm pf}$ are shown in Fig. 2. The upper two panels show how deviations from the ideal relation depend on bulge mass for both $v_{\rm pf} = 300$ $\rm km\,s^{-1}$ and 500 $\rm km\,s^{-1}$, while the lower two panels show histograms of these deviations averaged over all bulge masses. We see in these lower panels that the distribution of deviations from the ideal relation is very non-Gaussian, with a tail extending to very low values of $\log_{10}(M_{\rm BH}/M_{\rm ideal,BH})$. For $v_{\rm pf} = 300$ $\rm km\,s^{-1}$, 2.6% of bulges have black holes with mass smaller than 20% of the ideal $m_{\rm BH} - m_{\rm b}$ value. For $v_{\rm pf} = 500$ $\rm km\,s^{-1}$ this fraction jumps to 18.9%. The rms width of this distribution is not a good statistical description of the scatter in the $m_{\rm BH} - m_{\rm b}$ relation since the rms is dominated by the noisy tail. We use instead a more robust measure of width. We calculate the widths that contain

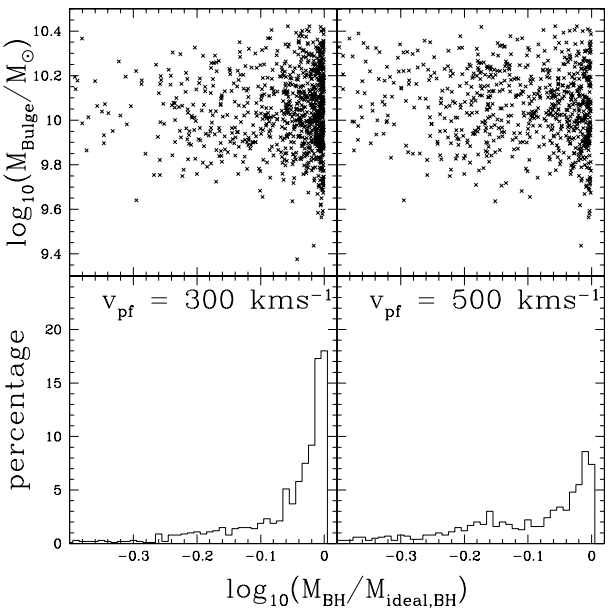

Figure 2. Top: residuals from the $m_{\rm BH} - m_{\rm b}$ relation. Plotted here is the dependence on bulge mass of the ratio of the black hole mass to the value for the 'ideal' $m_{\rm BH} - m_{\rm b}$ relation. Bottom: histogram of deviations from the ideal $m_{\rm BH} - m_{\rm b}$ relation.

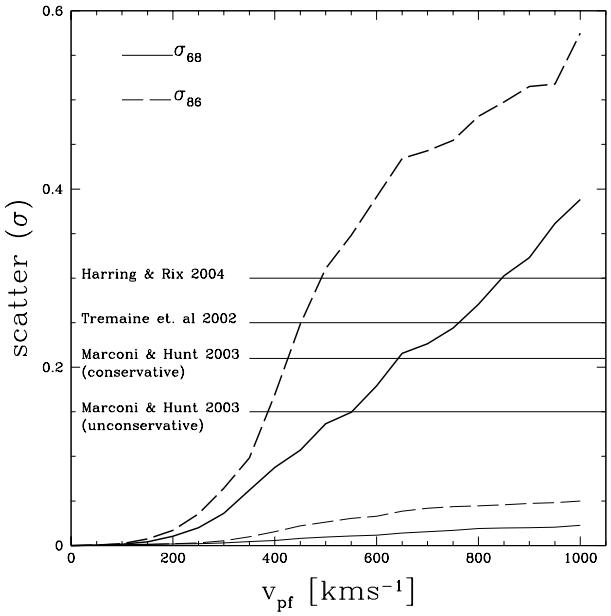

Figure 3. The scatter in the $m_{\rm BH} - m_{\rm b}$ relation as a function of the kick velocity prefactor, $v_{\rm pf}$. The curves show our estimates of the width of the distribution of $M_{\rm BH}/M_{\rm ideal,BH}$ induced by black hole ejections as discussed in the text. The solid and dashed curves represent σ_{68} and σ_{86} respectively. The thick lines show the estimates when disc instability produces bulges, while the thin lines represent models when this route for bulge formation is ignored. The horizontal lines show estimates of the scatter from various observational studies. Note that Tremaine et al. (2002) give only an upper limit, while Marconi & Hunt (2003) present two estimates to which they refer as conservative and unconservative.

68% and 86% of the distribution, and then define σ_{68} and σ_{86} to be half and one third of these widths respectively. For a Gaussian distribution both of these measures would equal σ, the usual rms width. Fig. 3 shows how these measures of scatter vary as a function of $v_{\rm pf}$ and compares them to published observational determinations. The non-Gaussian nature of the scatter results in the two curves being significantly different.

We immediately see that the contribution to the scatter in the $m_{\rm BH} - m_{\rm b}$ relation from ejected black holes is very sensitive to assumptions concerning disc stability. For the case where unstable discs are assumed to form bulges, large values of $v_{\rm pf}$ are strongly ruled out as they would produce more scatter in the $m_{\rm BH} - m_{\rm b}$ relation than is observed. Fig. 3 shows that to be consistent with the tightest observational limits (Tremaine et al. 2002; Marconi & Hunt 2003; Häring & Rix 2004) requires $v_{\rm pf} < 450$–$650\,{\rm km\,s^{-1}}$. This constraint is consistent with the kick velocities predicted by the general relativistic analysis of Favata et al. (2004) and Blanchet et al. (2005). Even so, if the prefactor velocity lies in the range $v_{\rm pf} = 300$ - $500\,{\rm km\,s^{-1}}$, as these calculations suggest, then gravitational recoil provides a substantial contribution to the scatter in the $m_{\rm BH} - m_{\rm b}$ relation.

In models where discs are assumed to be stable to the formation of a bulge, all the observational estimates of the scatter lie well above the values that result from recoiling black hole ejections. In this case, we conclude that even kicks with velocities exceeding the range expected from current calculations do not produce a significant contribution to the scatter in the $m_{\rm BH} - m_{\rm b}$ relation. There are two reasons for such a large difference between the two models. Firstly, when discs are assumed to be stable there are far fewer ($\sim 10\%$) bulge-bulge mergers and far more disc-bulge and disc-disc mergers involved in the formation of the galaxy. While the total number of mergers is the same in both models, the effect of the gravitational recoil depends only on the number of bulge-bulge mergers because, in our model, black holes only grow if there is a stellar spheroid.

The second reason for the difference between the two cases is that when discs are assumed to be stable, most ejections occur at early times ($z \approx 2$) when the bulges were smaller. The bulge then has enough time to regrow a black hole of the appropriate mass by subsequent galaxy mergers from which black hole ejection becomes increasingly difficult. When unstable discs are assumed to form bulges, the majority of the ejections occur much later ($z \lesssim 1$) and subsequent mergers are unable to grow a large black hole. Note that no black holes are ejected at $z < 0.7$ and $z < 0.3$ for disc-stable and disc-unstable models respectively.

5 THE BLACK HOLE DISTRIBUTION FROM N-BODY SIMULATIONS

In this section, we use high resolution N-body simulations of galactic halos to track the location of subgalactic and galactic black holes as the halo grows by mergers. The simulations provide spatial information that is not available in Monte-Carlo merger trees. We first describe the simulations and the way in which we model black hole escapees.

	$N_{\rm tot}$ (10^6)	$N_{\rm hr}$ (10^6)	$R_{\rm vir}$ (h^{-1} Mpc)	$N_{\rm vir}$ (10^6)
gh1	14.6	12.9	0.110	1.07
gh2	18.1	16.2	0.131	1.74
gh3	18.0	16.2	0.170	3.73
gh6	25.5	22.2	0.169	3.76
gh7	19.2	17.3	0.156	2.99
gh10	13.4	12.1	0.133	1.86

Table 1. Parameters for the six N-body halo simulations. The columns give: (1) halo label; (2) total number of particles in the simulation cube; (3) number of high resolution particles; (4) virial radius of the halo in h^{-1} Mpc defined as the distance from the centre to the radius at which the mean interior density is 200 times the critical density; (5) number of particles within the virial radius. All halos were simulated in a cube of comoving length $35.325\,h^{-1}$Mpc in a ΛCDM universe, with a particle mass of $2.64 \times 10^5 h^{-1} M_\odot$ in the 'high resolution' region.

5.1 Galaxies in the N-body simulations

We have used six N-body simulations of galactic-size dark matter halos of final mass $\sim 10^{12} M_\odot$ to study the demographics and spatial distribution of their black hole population, including black hole ejections. The simulations were performed using the GADGET code (Springel et al. 2001) in a flat ΛCDM universe with $\Omega_{\rm m} = 0.3, h = 0.7, \sigma_8 = 0.9$. These simulations have been previously studied by other authors (Power et al. 2003; Hayashi et al. 2004; Navarro et al. 2004; Libeskind et al. 2005) and we refer the reader to these papers for technical details. Briefly, each simulation follows the formation of structure in a cube of comoving side 35.325 h^{-1}Mpc with a Lagrangian 'high resolution" region around the halo of interest in which the particle mass is $2.64 \times 10^5 h^{-1} M_\odot$ and 'low resolution' particles elsewhere. Table 1 summarises the parameters of our six simulations.

Halos and their substructures were identified using the algorithm SUBFIND (Springel et al. 2001). The algorithm first identifies "friends-of-friends" groups using a linking length of 0.2 times the mean interparticle separation which approximately selects particles lying within the virialized region of the halo (Davis et al. 1985). Only halos with more than 10 particles, corresponding to a mass of $2.64 \times 10^6 h^{-1} M_\odot$, are considered. Then, using an excursion set approach, SUBFIND identifies self-bound subgroups within each friends-of-friends halo.

We use the method described by Harker et al. (2005) to construct full merger histories for the dark matter halos. Progenitor and descendant halos are identified at every timestep and tracked throughout the simulation in order to build the merger tree. The semi-analytic galaxy formation code GALFORM (e.g see Cole et al. 2000; Benson et al. 2002; Baugh et al. 1998) is then applied along each branch of each merger tree to obtain the properties of the central galaxy in each halo and its orbiting satellites. If the subhalo that hosts a satellite survives inside the parent halo, the position of the satellite is identified with the most bound subhalo particle. Some subhalos, however, are disrupted by tidal forces as they sink by dynamical friction and can no longer be identified by SUBFIND. In this case, the satellite is placed at the centre of mass of the particles that made up the subhalo at the last time it was identified. If the harmonic radius of these particles becomes greater than the distance between the satellite and the centre of the parent halo, the satellite is deemed to have merged into the central galaxy.

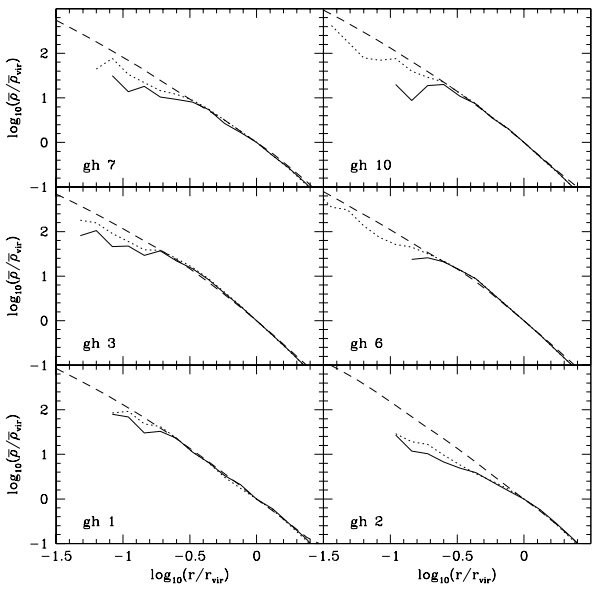

Figure 4. The mean interior radial dark matter density profiles for six simulated halos plotted against radius in units of the virial radius, and normalised to the value of the mean interior density at the virial radius (long dashed curve). The solid curves show the mean interior number density of satellites as a function of radius, normalised to the value at the virial radius. The dotted curve shows the mean interior density of all black holes (both those residing in satellites as well as the wandering ones), normalised to the value at the virial radius, assuming a kick velocity, $v_{\rm pf} = 300$ kms^{-1}.

Fig. 4 shows the spherically averaged dark matter density profile of our six halos normalised to the mean dark matter density within the virial radius. The galactrocentric distance is plotted in units of the virial radius (see Table 1). We also plot the corresponding number density profile of satellite galaxies with a V band magnitude $M_V < -7$. The dark matter profile follows the NFW form Navarro, Frenk & White 1996, 1997 quite closely (see Navarro et al. 2004). The radial distribution of the satellites is shallower than that of the dark matter in the inner parts of the halo. This result is broadly in agreement with the density distributions of substructures previously obtained from high resolution N-body simulations (see e.g Ghinga et al. 1998, 2000; Gao et al 2004). Note, however, that the profiles in Fig. 4 refer to satellite galaxies, not substructures and that 19.3% of the satellites are not attached to a subhalo. Nevertheless, the radial profile of the satellites is similar to that of subhalos.

5.2 The black hole population

The growth of galactic bulges and their associated black holes is calculated along each branch of the merger tree as described in Section 3.3. At the final time, each central galaxy contains a black hole typically of mass $10^7 h^{-1} M_\odot$ for

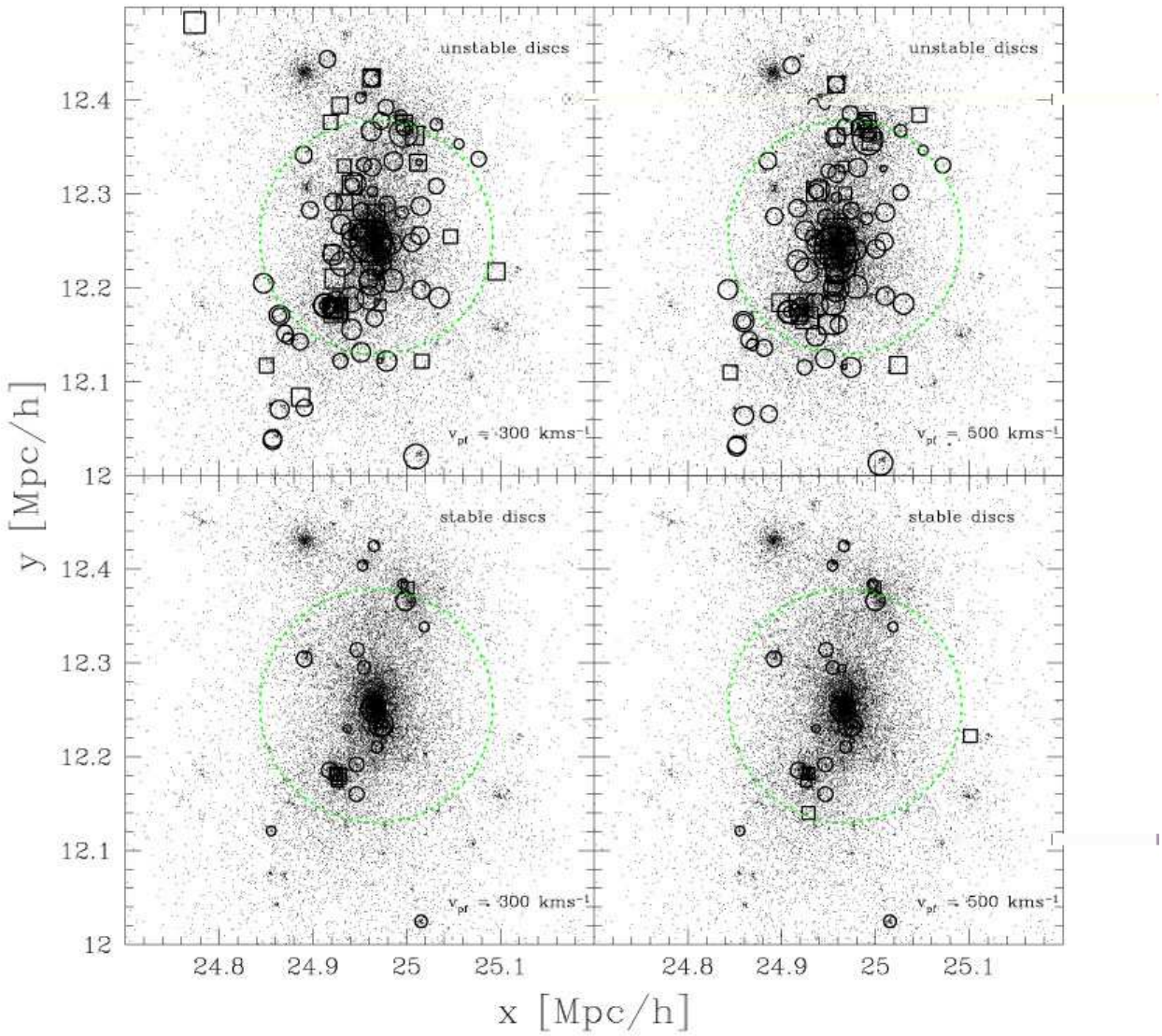

Figure 5. The spatial distribution of mass and black holes in simulation gh2. The top two panels correspond to the model in which unstable discs produce bulges, while the lower two panels correspond to the model in which this bulge formation channel is ignored. The left-hand and right-hand panels correspond to kick velocity prefactors of $v_{\rm pf} = 300\ {\rm km\,s^{-1}}$ and $v_{\rm pf} = 500\ {\rm km\,s^{-1}}$ respectively. Black holes are represented by symbols whose area is proportional to their mass. The open circles denote black holes that lie at the centre of a satellite galaxy, while open squares denote wandering black holes that were ejected during a merger. The central galactic supermassive black hole is in the middle of each panel. The virial radius of the halo is indicated by the dashed circle. The subset of intergalactic black

models where unstable discs form bulges and $10^6 h^{-1} M_\odot$ for models where disc instability is ignored. There are, in addition, two other populations of black holes. Firstly, there are "galactic black holes" that reside in the bulges of satellites in the halo; secondly, there are black holes that have been ejected from their host galaxy and which we term "wandering" black holes. The population of wandering black holes, in turn, is made up of "intrahalo black holes" that are still inside the host halo's virial radius at $z = 0$, and "intergalactic black holes" which have been ejected from the halo and lie outside the virial radius at $z = 0$.

5.2.1 Tracking black holes

Black holes that remain within their host bulge are always assumed to be located at the centre of the galaxy. When a black hole is ejected from its galaxy as a result of a recoil, we search for a particle in the simulation in the neighbourhood of the galaxy with appropriate velocity which, we assume, tracks the orbit of the black hole. To find as close a match as possible, we define a cost function and attach the escaping black hole to the particle that minimises the cost. The cost function we adopt is:

$$C_i^2 = \left(\frac{v_{\rm ej} - v_{i,\hat{r}}}{v_{i,\hat{r}}} \right)^2 + \left(\frac{\Delta r_i}{r_\star} \right)^2, \qquad (12)$$

where Δr_i and $v_{i,\hat{r}}$ are the position and radial velocity of the ith particle relative to the initial black hole position and velocity, $v_{\rm ej} = (v_{\rm kick}^2 - v_{\rm esc}^2)^{1/2}$ is the velocity the black hole has when it escapes from the galaxy and $r_\star = 0.33$ Mpc.

For modest kick velocities, $v_{\rm pf} \lesssim 300\ {\rm km\,s^{-1}}$, a suitable particle is usually found and 75% of the ejected black holes are identified with particles with $C_i < 0.5$. As $v_{\rm pf}$ is increased, the identification becomes increasingly difficult. Black holes with such large kick velocities, however, are likely to be ejected from the halo in any case. Thus, if no particle with $C_i < 0.5$ is found, we assume that the black hole has been lost from the halo to become part of a population of intergalactic black holes.

The general properties (number density, luminosity function) and spatial distribution of the satellite population depend somewhat on whether or not we assume that unstable discs generate galactic bulges. The statistics of the associated black holes, on the other hand, depend strongly on this assumption since many more bulges and black holes are formed when disc instability is taken into account. As above, in what follows, we take the unstable disc case as our fiducial model, but summarise also results when only mergers are assumed to give rise to bulges.

5.2.2 The distribution of black holes

The spatial distribution of black holes and dark matter in one of our simulations is illustrated in Fig. 5. The top two panels correspond to the model with unstable discs and the lower two to the model without unstable discs. In both cases, the left-hand column shows results for a kick velocity prefactor of $v_{\rm pf} = 300\ {\rm km\,s^{-1}}$ and the right-hand column for a kick velocity prefactor of $v_{\rm pf} = 500\ {\rm km\,s^{-1}}$. The greater efficiency of bulge formation in the unstable disc case is reflected in the larger number of black holes in this model. Those black holes that are still associated with a satellite galaxy are indicated by circles while those that have been ejected (the "wandering" black holes) are indicate by squares.

Tests of the mass resolution of our calculation in which we artificially increased the minimum halo mass used in the merger trees indicate that our catalogues are essentially complete for satellite galaxies with V-band luminosity brighter than -7 (corresponding to a mass larger than $1.4 \times 10^5 h^{-1} M_\odot$). To this limit we find that, for the unstable disc model, each simulated galaxy halo at $z = 0$ contains, on average, 52 satellites within its virial radius. The median bulge stellar mass of this population is $6.5 \times 10^6 h^{-1} M_\odot$ with a corresponding black hole mass of $6.5 \times 10^3 h^{-1} M_\odot$ in the ideal $m_{\rm BH} - m_{\rm b}$ relation. The fraction of these satellites that retain a central black hole at the final time depends weakly on the assumed prefactor for the kick velocities. For $v_{\rm pf} \lesssim 300\ {\rm km\,s^{-1}}$ 85.4% of satellites retain a central black hole at the final time, but this fraction is reduced to 84.2% for $v_{\rm pf} \lesssim 500\ {\rm km\,s^{-1}}$.

The number density profiles of the black hole populations of each of our simulations, assuming our fiducial $v_{\rm pf} = 300\ {\rm km\,s^{-1}}$, are shown by the dotted lines in Fig. 4. These can be compared with the dark matter density profiles and the corresponding number density profiles of satellite galaxies with a V band magnitude $M_V < -7$. In order to compare wandering and satellite black hole populations of similar masses, for this plot we selected only black holes with mass greater than that of the black hole in the lowest mass bulge of the satellite sample. The density profile of black holes is seen to be intermediate between that of the dark matter and that of the satellites and, in a couple of cases, wandering black holes are found as far in as $r_{\rm vir}/30$. Our understanding of this behaviour is that these black holes are ejected from the progenitors of both present day satellite galaxies and the progenitors of galaxies which by the present have merged with the central galaxy. As the ejection velocities are not large, these wandering black holes initially have orbits similar to the galaxies that ejected them but, being lighter, they are not subject to dynamical friction and so, unlike the satellite galaxies, those near the centre are not removed by merging with the central galaxy.

5.2.3 The black hole mass function

In the case of the fiducial model (in which unstable discs form bulges), each Milky-Way mass halo generated on average 80 black holes of mass greater than $10^2 h^{-1} M_\odot$ for $300 \lesssim v_{\rm pf} \lesssim 500\ {\rm km\,s^{-1}}$ during the course of its formation. Of these, at $z = 0$ approximately half were wandering black holes and the other half were galactic black holes retained by their host satellite galaxies. Of the wandering black holes, the fraction that are ejected with sufficient velocity to completely escape the halo depends more sensitively on $v_{\rm pf}$. For $v_{\rm pf} = 300\,{\rm km\,s^{-1}}$, 42% become intergalactic wandering black holes while for $v_{\rm pf} = 500\,{\rm km\,s^{-1}}$ this fraction increases to 60%. These numbers and the corresponding ones for the model in which disc instability is ignored are given in Table 2.

At the present day, there are only 50 black holes more massive than $10^2 h^{-1} M_\odot$ within the central 100 h^{-1}kpc of the halo. Black hole passages through the disc are therefore rare and unlikely to have affected the structure of the disc

Table 2. The mean number of satellite galaxies and black holes for both the fiducial model in which unstable discs form bulges and the model in which disc instability is ignored. In all cases we only consider satellites within $r_{\rm vir}$ with $M_v < -7$ and black holes with $M_{\rm BH} > 10^2 h^{-1} M_\odot$. The first section of the table lists the mean number of satellites with bulges and their median and minimum total stellar masses. The second section lists, for both $v_{\rm pf} = 300$ km s^{-1} and $v_{\rm pf} = 500$ km s^{-1}, the mean total number of black holes within the virial radius, $\bar{\rm N}_{\rm BH}$, of which $\bar{\rm N}_{\rm satBH}$ are galactic black holes residing in satellite galaxies, and $\bar{\rm N}_{\rm intrahaloBH}$ are wandering black holes within the main galaxy halo. The last row gives $\bar{\rm N}_{\rm intergalacticBH}$, the mean number of wandering black holes that have escaped beyond the virial radius of the main halo.

	Stable discs		Unstable discs	
$\bar{\rm N}_{\rm sat}$ with bulges	17.3		52.5	
Median $M_{\rm blg}$	$2.42 \times 10^6 h^{-1} M_\odot$		$6.5 \times 10^5 h^{-1} M_\odot$	
Smallest $M_{\rm blg}$	$1.68 \times 10^5 h^{-1} M_\odot$		$1.4 \times 10^5 h^{-1} M_\odot$	
	300 km s^{-1}	500 km s^{-1}	300 km s^{-1}	500 km s^{-1}
$\bar{\rm N}_{\rm BH}$	17.3	17.0	64.5	59.3
$\bar{\rm N}_{\rm satBH}$	15.2	15.2	44.0	43.3
$\bar{\rm N}_{\rm intrahaloBH}$	2.2	1.8	20.5	16.0
$\bar{\rm N}_{\rm intergalacticBH}$	3.2	4.0	15.0	23.5

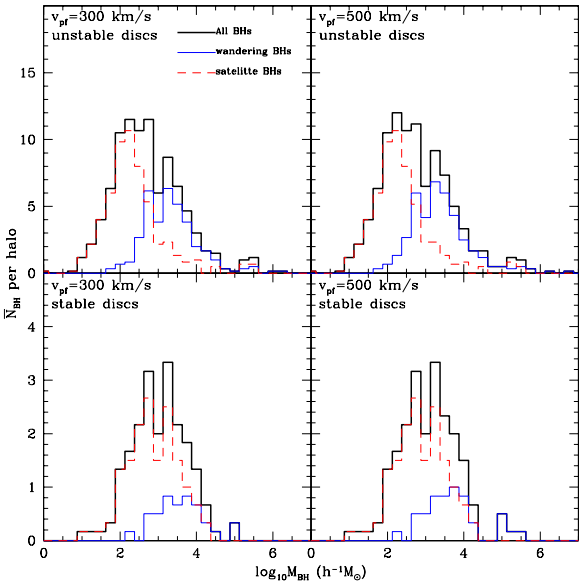

Figure 6. The total mass functions for halo black holes. The left hand panel shows the average number of black holes per halo for $v_{\rm pf} = 300$ km s^{-1} while the right hand panel shows the same quantity for $v_{\rm pf} = 500$ km s^{-1}. The upper two panels show histograms for models where discs are unstable to bulge formation while the bottom two panels show data for models where instability is ignored. The red dashed histogram represents the mass function of black holes that reside in satellite galaxies; the blue solid histrogram represents the mass function of wandering black holes that have been ejected from their host bulges. The black histogram is the combined mass function.

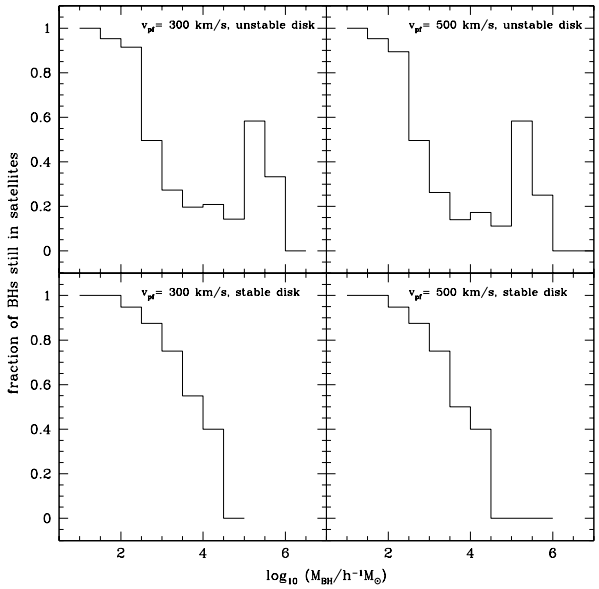

Figure 7. The fraction of black holes that remain in satellites as a function of black hole mass. The left two panels are for $v_{\rm pf} = 300$ km s^{-1}, the right two are for $v_{\rm pf} = 500$ km s^{-1}. The upper two panels are for unstable disc models, while the lower two panels are for stable disc models.

substantially. A large population of intergalactic black holes exists beyond the virial radius of the halo. Some of these are attached to small galaxies that will eventually become satellites, but others are black holes that were ejected from the halo altogether. (Only the fraction of these that were tagged with a particle are shown in Fig. 5.)

Fig. 6 shows the mass function of halo black holes, averaged over all six simulations, for two assumed values of $v_{\rm pf}$ in the models with and without unstable discs. Black holes in satellites within the virial radius whose host galaxy is brighter then $M_V < -7$ and all wandering black holes are included. In all cases, the central supermassive black hole of mass $\sim 10^6 - 10^7\, M_\odot$ has been omitted from the sample. In the unstable disc case, the medians of the distribution are $10^{2.52} h^{-1} M_\odot$ and $10^{2.56} h^{-1} M_\odot$ for $v_{\rm pf} = 300$ and 500 km s^{-1} respectively. In both cases, we expect a typical halo to have ~ 3 black holes of mass $M > 10^5 h^{-1} M_\odot$. The mass distribution is slightly wider for the larger value of $v_{\rm pf}$, reflecting the larger efficiency of black hole ejection in this case. In the case where disc instabilities are ignored,

their are fewer black holes (note the difference in the scales of the y-axes in the upper and lower panels of this figure), but the distributions are shifted to slightly higher black hole masses with a median of $\sim 10^{3.0}h^{-1}M_{\odot}$ and virtually no black holes of mass $M > 10^5 h^{-1}M_{\odot}$. The reason why the median is shifted to slightly higher masses in the stable disc case is because in this case there are fewer ejections, thus allowing satellite galaxy black holes to grow larger.

Also shown in Fig. 6 is the result of splitting the black hole mass function into the two populations: the satellite galaxy black holes and wandering black holes (red dashed and blue solid line respectively). The bimodal nature of the total mass function is visible as the result of these two distinct populations. The median of the satellite black hole mass distribution is $\sim 10^{2.24}h^{-1}M_{\odot}$ while the wandering black hole population peaks at $\sim 10^{3.25}h^{-1}M_{\odot}$ for unstable disc modes. In the stable disc models, the bimodality is also visible although slightly less pronounced. This tendency for the wandering black holes to be more massive than those retained in the satellites is shown clearly in Fig. 7, which plots the fraction of black holes of each mass that are associated with satellite galaxies as a function of black hole mass. We see that below $10^5 M_{\odot}$ the fraction associated with satellite galaxies is a decreasing function of black hole mass. For low masses ($M < 10^{2.5}h^{-1}M_{\odot}$), more than 90% of black holes are in satellites. However, at higher masses ($10^{3.5} < M < 10^5 h^{-1}M_{\odot}$), the majority of black holes are found to be wandering. The reason for this bias in the masses of wandering black holes compared to satellite black holes is the fact that larger satellites are more likely to merge and experience a kick then smaller ones. Since the dynamical friction timescale is inversely dependent on satellite mass (eq. 4.16 in Cole et al. 2000), we expect the physics of kicks to have a larger effect on the higher mass satellites and bulges than on the lower mass ones. The lower mass satellites will have experienced few if any ejections and their central black holes will be unaffected by velocity kicks.

In principle, a large population of wandering black holes could affect the match between the total mass in black holes at the present day and the mass in quasar remnants inferred from energy considerations (Soltan 1982). In our calculations, however, wandering black holes make up, on average, only 2.6% and 3.9% of the total black hole mass in our simulated galactic halos for $v_{\rm pf} = 300\,{\rm km\,s^{-1}}$ and $500\,{\rm km\,s^{-1}}$ respectively. Wandering black holes do, however, make up a large fraction of the intrahalo black hole population (ie. all halo black holes excluding the central one). For these two values of $v_{\rm pf}$, unattached wandering intrahalo black holes make up 31.8% and 48.4% of the total intrahalo satellite black hole mass.

Another noteworthy feature of the black hole mass functions of Fig. 6 is the small population of very massive black holes with $M_{\rm BH} > 10^5 h^{-1}M_{\odot}$. This population is primarily composed of wandering black holes, although a portion of it in the unstable disc model consists of black holes in massive satellites whose bulge masses are $\sim 10^{8.24}h^{-1}M_{\odot}$, as evidenced by the high mass peak in the upper panels of Fig. 7. In stable disc models, this population is composed entirely of wandering black holes. These massive wandering black holes originate from ejections from the central galaxy that occured when the central galaxies bulge had a mass of $\sim 10^9 h^{-1}M_{\odot}$. The central galaxy has since undergone subsequent phases of bulge formation to bring its mass to $\sim 10^{10}h^{-1}M_{\odot}$ and, in the process, has regrown a central black hole of mass $\lesssim 10^7 h^{-1}M_{\odot}$.

6 DISCUSSION AND CONCLUSIONS

The gravitational recoil of merging black holes is an important physical effect in a universe built up hierachically through the repeated merging of galactic units. Whenever galaxies that host black holes merge, the black holes themselves will coalesce and there exists the potential for the remnant black hole to be ejected from the galaxy, provided the recoil velocity is high enough and the galactic potential shallow enough.

We have examined the role that gravitational recoil plays on the demographics of black holes. We find that the process of ejecting black holes from galaxies is efficient if bulges and black holes grow both in galaxy mergers and as a result of discs becoming unstable, because in this case nearly all bulges contain a black hole. In models where disc instability is ignored, this process is not as efficient because fewer bulges and associated black holes exist and because black hole - black hole mergers tend to occur late when the galactic potential wells are deeper. In the former case, black hole ejections produce a significant contribution to the scatter in the $m_{\rm BH} - m_{\rm b}$ relation. In fact, conservative estimates of the scatter in the observed relation constrain the recoil prefactor velocity to $v_{\rm pf} < 500\,{\rm km\,s^{-1}}$, which is consistent with the general relativitistic calculations of Favata et al. (2004) and Blanchet et al. (2005).

Is there any empirical evidence for the kind of black hole processes present in our model? Coccato et al. (2005) have recently reported the discovery of a black hole in NGC 4435 whose mass is smaller than about 20% of the value expected from the $m_{\rm BH} - m_{\rm b}$ relation. Black holes with a smaller than expected mass arise naturally in our model, although masses as extreme as this could be rare. For example, in our model with $v_{\rm pf} = 300\,{\rm km\,s^{-1}}$, only $2-3\%$ of black holes have a mass that deviates as much or more from the mean relation as that of the black hole in NGC 4435. However, if $v_{\rm pf} = 500\,{\rm km\,s^{-1}}$ this fraction raises to $\sim 20\%$.

Indirect evidence for black holes with masses below those expected from the $m_{\rm BH} - m_{\rm b}$ relation has been presented by Colbert & Mushotzky (1999). They argue that the compact X-ray sources often seen near the centre of elliptical and spiral galaxies could be black holes of mass $\sim 10^2 - 10^4 M_{\odot}$. Interestingly, these sources are often displaced from the centre by a few hundred parsecs. Similarly, Neff et al. (2003) have discovered a group of off-centre compact X-ray sources in the merger remnant NGC 3256 which, they argue, could be intermediate-mass black holes. In our model, these objects might be identified with the black holes of infalling satellites or with recently merged black holes that have been kicked out of the galactic centre, their growth stunted as a result.

To investigate the spatial distribution of black holes in Milky-Way like galactic halos we used a set of N-body simulations to track both the satellite galaxies that host black holes and also the black holes that are ejected from their host galaxies. We find that the black hole mass function is bimodal, being composed of two overlapping populations.

The lower mass population consists of black holes at the centre of orbiting low mass satellites that have not undergone recent mergers, while the slightly higher mass population is composed of wandering black holes that have been ejected from mergers that formed the central galaxies and the more massive satellites. Among the latter population, we find a few supermassive ($< 10^6 h^{-1} M_\odot$) black holes that were ejected from the main progenitor of the central galaxy sufficiently early such that the bulge of the central galaxy has had enough time to regrow a sizable black hole. There is also an intergalactic population consisting of black holes whose recoil velocity was large enough not only to unbind them from their host galaxy but also from its halo.

In the future it may be possible to detect the formation of wandering black holes directly using instruments such as *LISA*[1] that can directly measure the gravitational radiation emitted in the black hole – black hole merger that ejects the remnant. In the meantime, detecting these black holes presents an interesting challenge. In practice, an ejected intergalactic or intrahalo black hole is likely to bring along a small cusp of stars tightly bound to it as it escapes the halo's potential. These stars would provide the only measurable way of detecting such black holes. Most likely, there would not be any gas that could be accreted and hence the black holes would not be observable in the conventional way. However, as the orbits of the stars which the black hole brought with it from the bulge decay, the stars may plunge into the black hole. In addition to emitting a burst of gravitational radiation, this type of infall would tidally disrupt the star and create a small accretion disc which would radiate according to the standard physics of accretion discs. The gravitational radiation signature and accretion disc emission would provide the best way to identify these black holes.

Magain et al. (2005) have recently discovered a quasar, HE0450-2958, which has no visible host galaxy and, at first sight, is a good candidate for an escaped black hole. Haehnelt, Davies & Rees (2005) have indeed suggested that the quasar may have been ejected from a nearby ultraluminous infrared galaxy (ULIRG) either through the gravitational recoil process we are considering here or through a gravitational slingshot associated with three or more black holes involved in the merger responsible for the ULIRG. However, Hoffman & Loeb (2005) have argued that the quasar is much too far from the companion galaxy to have been ejected with a velocity of 300 $\mathrm{km\,s^{-1}}$ and so favour a slingshot mechanism.

Ultraluminous X-ray sources (ULXS) or micro-quasars have long been regarded as candidates for intermediate-mass black holes, $M_{\rm BH} \sim 100 - 1000 M_\odot$, radiating near the Eddington limit (see e.g. Fabbiano 1989; Mushotzky 2004 and references therein). This is exactly the kind of object that would be naturally identified with the orbiting intrahalo black holes predicted by our model. This interpretation, however, has two difficulties. Firstly, ULXs tend to be associated with star-forming regions and their frequency seems to be correlated with the galactic star formation rate (see e.g. Ward 2005; Kaaret et al. 2004 and references therein). These facts lend support to the view that ULXs are stellar mass black holes emitting beamed radiation at highly super-Eddington rates. The second arguement against identifying ULXs with the intrahalo black holes in our model is the difficulty of finding a suitable source of material for the black hole to accrete. There are, however, some examples of ULX's, most notably the ULX in M82 (Kaaret et al. 2001), that are probably much too bright to be explained even as exotic super-Eddington luminosity stellar mass black holes (King et al. 2001). King & Dehnen (2005) call objects like this "Hyperluminous X-ray sources" (HLX) and argue that these objects are precisely the intrahalo black holes associated with satellites in our model which switch on when they come close to the galactic centre. Since the exact mechanism by which these black holes would be activated is uncertain, we cannot predict how common this phenomenon should be. However, our model contains, in principle, a plentiful supply of intermediate mass black holes orbiting in the halo of every galaxy which is sufficient to account for the presence of a few ULXs or HLXs in most galaxies.

[1] `http://lisa.jpl.nasa.gov/`

REFERENCES

Baugh C. M., Cole S., Frenk C. S., Lacey C. G., 1998, ApJ, 498, 504

Benson A. J., Lacey C. G., Baugh C. M., Cole S., Frenk C. S., 2002, MNRAS, 333, 156

Benson A. J., Frenk C. S., Baugh C. M., Cole S., Lacey C. G., 2003, MNRAS, 343, 679

Binney, J. & Tremaine, S., 1987 Galactic Dynamics. Princeton University Press, New Jersey.

Blanchet L., Qusailah M. S. S., Will C. M., 2005 ApJ accepted

Bower R. G., Benson A. J., Malbon R., Helly J. C., Frenk C. S., Baugh C. M., Cole S., Lacey C. G., submitted to MNRAS, preprint (astro-ph/0511338)

Cattaneo A., Haenhelt M., Rees M. J., 1999 MNRAS 308,77

Coccato, L., Sarzi, M., Pizzella, A., Corsini, E.M., dall Bonta, E. & Bertola, F., 2005, submitted to MNRAS (astro-ph/0511696).

Cole, S., Lacey, C. G., Baugh, C. M., Frenk, C. S. 2000 MNRAS, 319, 168

Colbert E., Ptak A., 2002 ApJS 143, 25

Colbert E., Mushotzky R., 1999 ApJ, 519, 89

Croton D. J., Springel V., White S. D. M., Lucia G. De, Frenk C. S., Gao L., Jenkins A., Kauffmann G., Navarro J. F., Yoshida N. 2005 MNRAS, in press, preprint (astro-ph/0508046)

Davis M., Efstathious G., Frenk C. S., White S. D. M., 1985, ApJ, 292, 371

Di Matteo T., Springel V., Hernquist L., 2005 Natur., 433, 604

Efstathiou, G., Lake, G., Negroponte, J. 1982 MNRAS, 199, 1069

Enoki M., Inoue K. T., Nagashima M., Sugiyama N., 2004 ApJ, 615, 19

Fabbiano G., 1989 ARA&A, 27, 87

Favata, M., Hughes, S. A., Holz, D. E. 2004 ApJ, 607, L5

Ferrarese, L. & Merritt, D. 2000 ApJ 539,L9

Fitchett, M. J. 1983 MNRAS, 203, 1049

Gao L., White S. D. M., Jenkins A. Stoehr F., Springel V., 2004 MNRAS 355, 819

Gebhardt, K., Bender, R., Bower G., et al, S. 2000 ApJ, 539, L13
Gebhardt K., Rich R. M., Ho L. C., 2002 ApJ 578, L41
Ghigna S., Moore B., Governato F., Lake G., Quinn T., & Stadel, J. 2000 ApJ 544,616
Ghigna, S., Moore B., Governato F., Lake G., Quinn T., Stadel J. 1998 MNRAS,300,146
Graham A. W., Erwin P., Caon N., Trujillo I., 2001 ApJ, 563, L11
Härring N., Rix H. W., 2004 ApJ, 604, L89
Haehnelt M. G., Rees M. J. 1993 MNRAS 263, 178
Haehnelt M. G., Davies, M. B., Rees M. J. 2005 MNRAS in press (astro-ph/0511245)
Harker, G., Cole, S. M., Helly, J. H. Frenk, C. S. & Jenkins, A.R. 2005, submitted to MNRAS, (astro-ph/0510488)
Hayashi E., Navarro J. F., Power C., Jenkins A., Frenk C. S., White S. D. M., Springel V., Stadel J., Quinn T., 2004, MNRAS, 355, 794
Helly J., Cole S., Frenk C. S., Baugh C. M., Benson A., Lacey C. G., 2003, MNRAS, 338, 903
Hernquist, L. 1990 ApJ, 356, 359
Hoffman L, Loeb A., Submitted to Nature. preprint (astro-ph/0511242)
Kaaret, P., Prestwich, A. H., Zezas, A., Murray, S. S., Kim, D.-W., Kilgard, R. E., Schlegel, E. M., Ward, M. J. 2001, MNRAS 321, 29
Kaaret P., Alonso-Herrero A., Gallagher J. S., Fabbiano G., Zezas A., Rieke M. J., 2004 MNRAS, 348, 28
Kauffman G., Haehnelt M., 2000 MNRAS, 311, 576
King, A. R. & Dehnen, W. 2005, MNRAS, 357, 275
King A. R., Davies M. B., Ward M. J., Fabbiano G., Elvis M., 2001, ApJ, 552, L109
Kormendy, J., & Richstone, D. O. 1995, ARA&A, 33, 581
Magain P., Letawe G., Courbin F., Jablonka P., Jahnke K., Meylan G.,Wisotzki L., 2005 Nature, 437, 381
Lacey, C. G., Cole, S. 1993 MNRAS, 262, 627
Libeskind N. I., Frenk C. S., Cole S., Helly J. C., Jenkins A., Navarro J. F., Power C., 2005 MNRAS, 363, 146
Madau, P., & Quataert 2004, ApJL, 606, L17
Magorrian, J., Tremaine, S., Richstone, et al. 1998, AJ, 115, 2285
Marconi, A., & Hunt, L. K. 2003 ApJ, 589, L21
Malbon R., in prep
McLure, R. J., & Dunlop, J. S. 2002, MNRAS, 331, 795
Menou K., Haiman Z., Narayanan V. K., 2001 ApJ, 558, 535
Mo, S., Mao, H. & White, S.D.M. 1998, MNRAS, 295, 319
Merritt, D., & Ferrarese, L. 2001 MNRAS 320 L30
Merritt, D., Milosavlejevic, M., Favata, M., Hughes, S. A., & Holz, D., E. 2004 ApjL, 607, L9
Milosavljevic M., Merritt, D., 2001 ApJ, 563, 34
Mushotzky, R., 2004 Prog. Theor. Phys. Suppl. 155, 27-4
Navarro J. F., Frenk C. S., White S. D. M. 1996 ApJ, 462,563
Navarro J. F., Frenk C. S., White S. D. M. 1997 ApJ, 490,493
Navarro J. F., Hayashi E., Power C., Jenkins A., Frenk C. S., White S. D. M., Springel V., Stadel J., Quinn T., 2004, MNRAS, 349, 1039
Neff S. G., Ulvestad J. S., Campion S. D. 2003 ApJ 599, 1043
Ostriker J. P., 2000, PhRvL, 84, 5258O
Peres A., 1962, PhRv, 128, 2471
Peters P. C., Matthews J., 1963, Ph Rv, 13,1 435
Power C., Navarro J. F., Frenk C. S., Jenkins A., White S. D. M., Springel V., Stadel J., Quinn T., 2003, MNRAS, 338, 14
Saslaw W. C., Valtonen M. J., Aarseth, S. J., 1974 ApJ 190, 253
Silk J., Rees M. J., 1998, A&A, 331, L1
Soltan, A. 1982, MNRAS, 200, 115
Springel, V., Yoshida, N. & White, S. D. M. 2001a *New Astronomy*, 6, 51
Springel, V., White, S. D. M., Tormen, G. & Kauffmann, G. 2001b MNRAS, 328, 726
Tasca L. A. M., White S. D. M, submitted to MNRAS. preprint (astro-ph/0507249)
Tremaine, S., Gebhardt, K., Bender, R. et al 2002 ApJ, 574, 740
Volonteri M., Haardt F., Madau P., 2003 ApJ 582, 559
Ward M. 2005, to appear in Meurs E. J. A., Fabbiano G., eds, Proc. IAU Symp. 230 Populations of High Energy Sources in Galaxies